Coupling δ^2H and $\delta^{18}O$ biomarker results yields information on relative humidity and isotopic composition of precipitation – a climate transect validation study

M. Tuthorn[1], R. Zech[2], M. Ruppenthal[3], Y. Oelmann[3], A. Kahmen[4], H. F. del Valle[5], T. Eglinton[2], K. Rozanski[6], M. Zech[1,7,*]

[1)] Department of Soil Physics and Chair of Geomorphology, University of Bayreuth, Universitätsstr. 30, D-95440 Bayreuth, Germany

[2)] Geological Institute, ETH Zurich, Sonneggstrasse 5, CH-8092 Zurich, Switzerland

[3)] Geoecology, University of Tübingen, Rümelinstr. 19-23, D-72070 Tübingen, Germany

[4)] Department of Environmental Sciences - Botany, University of Basel, Schönbeinstrasse 6, CH-4056 Basel, Switzerland

[5)] Ecología Terrestre, Centro Nacional Patagónico (CENPAT), Consejo Nacional de Investigaciones Científicas y Técnicas (CONICET), Boulevard Brown 2825, U9120ACF Puerto Madryn, Argentina

[6)] Faculty of Physics and Applied Computer Science, AGH University of Science and Technology, Kraków, Al. Mickiewicza 30, 30-059 Kraków, Poland

[7)] Institute of Agronomy and Nutritional Sciences, Soil Biogeochemistry, Martin-Luther University Halle-Wittenberg, von-Seckendorff-Platz 3, D-06120 Halle, Germany

*) corresponding author (michael_zech@gmx.de)

Abstract

The hydrogen isotopic composition (δ^2H) of leaf waxes, especially of *n*-alkanes ($\delta^2H_{n\text{-alkanes}}$), is used increasingly for paleohydrological and –climate reconstructions. However, it is challenging to disentangle past changes in the isotopic composition of precipitation and changes in evapotranspirative enrichment of leaf water, that are both recorded in leaf wax δ^2H values. In order to overcome this limitation, Zech M. et al. (2013, Chemical Geology 360-361, pp. 220-230) proposed a coupled $\delta^2H_{n\text{-alkane}}$-$\delta^{18}O_{sugar}$ biomarker approach. This coupled approach allows calculating (i) biomarker-based 'reconstructed' $\delta^2H/\delta^{18}O$ values of leaf water ($\delta^2H/\delta^{18}O_{leaf\ water}$), (ii) biomarker-based 'reconstructed' deuterium excess (d-excess) of leaf water, which mainly reflects evapotranspirative enrichment and which can be used to reconstruct relative air humidity (RH) and (iii) biomarker-based 'reconstructed' $\delta^2H/\delta^{18}O_{precipitation}$ values.

Here we present a climate transect validation study by coupling new results from δ^2H analyses on *n*-alkanes and fatty acids in topsoils along a climate transect in Argentina with previously measured $\delta^{18}O$ results obtained for plant-derived sugars. Accordingly, both the reconstructed RH and $\delta^2H/\delta^{18}O_{precipitation}$ values correlate significantly and highly significantly, respectively, with actual RH and $\delta^2H/\delta^{18}O_{precipitation}$ values. We conclude that compared to single $\delta^2H_{n\text{-alkane}}$ or $\delta^{18}O_{sugar}$ records, the proposed coupled $\delta^2H_{n\text{-alkane}}$-$\delta^{18}O_{sugar}$ biomarker approach will allow more robust $\delta^2H/\delta^{18}O_{precipitation}$ reconstructions and additionally the reconstruction of mean summer daytime RH changes/history in future paleoclimate research.

Keywords: paleoclimate proxies, hemicellulose sugars, *n*-alkanes, leaf water enrichment, deuterium-excess, relative air humidity

1. Introduction

Long chain *n*-alkanes and fatty acids are important components of the epicuticular leaf waxes of terrestrial plants (Eglinton, 1967; Samuels et al., 2008). As leaf waxes can be preserved in sedimentary archives over a long time they serve as valuable biomarkers for paleo-environmental and -climate reconstructions (Eglinton and Eglinton, 2008; Zech M. et al., 2011b). The δ^2H isotopic composition of leaf waxes is of particular interest in this regard, because, at least to a first order, it reflects the isotopic composition of precipitation δ^2H_{prec} (Sauer et al., 2001; Huang et al., 2004; Sachse et al., 2004; Schefuss et al., 2005; Pagani et al., 2006; Tierney et al., 2008; Rao et al., 2009), which in turn depends on temperature, amount of precipitation, atmospheric circulation, etc. (Dansgaard, 1964; Rozanski et al., 1993; Gat, 1996; Araguas-Araguas et al., 2000). While there is probably no fractionation of hydrogen isotopes during water uptake by the roots (Ehleringer and Dawson, 1992), several studies have shown that leaf water is enriched in ^2H compared to the source water or precipitation (Flanagan et al., 1991; Yakir, 1992; Sachse et al., 2006; Smith & Freeman, 2006; Farquhar et al., 2007; Feakins & Sessions, 2010). This ^2H enrichment, which is also recorded in the leaf waxes (Kahmen et al., 2013a,b), can be explained by evapotranspiration and is mainly controlled by relative air humidity (RH), temperature and the isotopic composition of atmospheric water vapor. Indeed, a robust reconstruction of δ^2H_{prec} from soils and sedimentary records turns increasingly out to be quite challenging, because it is hitherto difficult to disentangle past changes in δ^2H_{prec} and changes in evapotranspirative enrichment of leaf water (Zech, R. et al., 2013; Zech, M. et al., 2015).

Compared to compound-specific δ^2H analyses, compound-specific $\delta^{18}O$ analyses are by far less adopted by the scientific community, so far (Hener et al., 1998; Juchelka et al., 1998; Jung et al., 2005; Jung et al., 2007; Greule et al., 2008). However, particularly compound-specific $\delta^{18}O$ analyses of hemicellulose-derived sugar biomarkers ($\delta^{18}O_{sugars}$) extracted from

plants, soils and sediments are proposed to have large potential especially in paleoclimate/-hydrologic research (Zech M. & Glaser, 2009; Zech M. et al., 2012). Similar to leaf waxes, hemicellulose-derived sugars record the isotopic composition of water used for metabolism, i.e. the isotopic composition of precipitation altered by evapotranspirative ^{18}O enrichment of soil and leaf water (Tuthorn et al., 2014; Zech M. et al., 2014a). Recently, Zech M. et al. (2013) proposed a conceptual coupled $\delta^2H_{n\text{-alkane}}$-$\delta^{18}O_{sugar}$ model for paleoclimate research and suggested that this coupling allows overcoming the above defined limitation of single $\delta^2H_{n\text{-alkane}}$ approaches. Accordingly, the coupled $\delta^2H_{n\text{-alkane}}$-$\delta^{18}O_{sugar}$ approach allows reconstructing (i) $\delta^2H/\delta^{18}O_{leaf\ water}$ values, (ii) deuterium excess (d-excess) of leaf water, which mainly reflects evapotranspirative enrichment and can be used to reconstruct relative air humidity (RH) and (iii) $\delta^2H/\delta^{18}O_{prec}$ values.

The study presented here aimed at evaluating the coupled $\delta^2H_{n\text{-alkane}}$-$\delta^{18}O_{sugar}$ biomarker approach by applying it to a modern topsoil climate transect from Argentina. More specifically, we aimed at (i) analysing and comparing the δ^2H values of *n*-alkanes and fatty acids, (ii) modelling ^2H leaf water enrichment along the transect and comparison of $\delta^2H_{leaf\ water}$ values with $\delta^2H_{n\text{-alkane}}$ and $\delta^2H_{fatty\ acid}$ values, (iii) reconstructing d-excess of leaf water using the coupled $\delta^2H_{n\text{-alkane}}$-$\delta^{18}O_{sugar}$ approach and evaluating the potential for reconstructing RH, and (iv) reconstructing 'biomarker-based' $\delta^2H/\delta^{18}O_{prec}$ values and comparison with actual $\delta^2H/\delta^{18}O_{prec}$ values.

2. Material and methods

2.1. Transect description and samples

The investigated transect in Argentina spans from ~32°S to 47°S, and encompasses 20 sampling locations spanning a large climate and altitudinal (22 – 964 m) gradient (Fig. 1). Mean annual temperature ranges from 11.4 °C to 18.0 °C and mean annual precipitation from

185 mm to 1100 mm (GeoINTA, 2012). Precipitation shows a systematic southward trend towards more negative $\delta^{18}O$ and $\delta^{2}H$ values ($\delta^{18}O_{prec}$ and $\delta^{2}H_{prec}$, respectively) (Bowen, 2012).

The transect is described in detail by Tuthorn et al. (2014) and Ruppenthal et al. (2015). Briefly, it is characterized by warm humid subtropical conditions in the north (Zárate, Buenos Aires Province), pronounced arid conditions in the middle part of the transect and cool temperate conditions in the south (Las Heras, Santa Cruz Province). These markedly contrasting climate conditions are reflected in the vegetation zones of the study area, changing from Humid/Dry Pampa (with dominance of *Triticum, Setaria, Eragrostis, Andopogon, Panicum* and *Festuca* species) in the north to the Espinal vegetation zone (with dominance of *Festuga and Larrea* species) that prevails under semi-arid climate (Burgos and Vidal, 1951), Low Monte semidesert/desert (with dominance of *Larrea* species) in the most arid region of Argentina (Fernández and Busso, 1997), and Patagonian Steppe (with dominance of *Stipa* species) in the southernmost part of the transect (Le Houérou, 1996; Paruelo et al., 1998).

During a field campaign in March and April 2010, mixed topsoil samples (A_h-horizons) from maximum 51 cm depth were collected in triplicate replication from the 20 sample sites along the transect (for soil type and total organic carbon contents please see Table 1 of Tuthorn et al., 2014). The soil samples were air-dried in the field and later in an oven at 50°C for several days. The sampling site heterogeneity was checked for the $\delta^{18}O_{sugar}$ analyses and in most cases did not exceed the analytical uncertainty (Table 2 in Tuthorn et al., 2014). Therefore, the field replications were merged to one composite sample per study site for $\delta^{2}H_{lipid}$ analyses.

2.2. Compound-specific $\delta^{2}H$ analyses of *n*-alkanes and fatty acids

For $\delta^{2}H$ analyses of *n*-alkane and fatty acid biomarkers, an Accelerated Solvent Extractor (Dionex ASE 200) was used to extract free lipids from the dried soil samples with dichloromethane (DCM) and methanol (MeOH; 9:1) according to Zech R. et al. (2013). The

total lipid extracts were separated over pipette columns filled with ~2 g aminopropyl. *n*-Alkanes were eluted with hexane, more polar lipids with DCM:MeOH (1:1), and free fatty acids with diethyl ether:acetic acid (19:1). The *n*-alkanes were further purified using zeolite (Geokleen) pipette columns. The zeolite was dried and dissolved in HF after eluting branched- and cyclo-alkyl compounds with hexane, and the straight-chain (n-alkyl) compounds were then recovered by liquid-liquid extraction with hexane. For samples 1 – 12, an additional purification step with silver nitrate columns was carried out in order to eliminate unsaturated compounds. The chromatograms of the other samples displayed no requirement for this purification step.

Fatty acids were methylated using 5% HCl in methanol at 80°C for 12 hours. Subsequently, liquid-liquid extraction with 5% NaCl and hexane was used to retrieve fatty acid methyl esters (FAMEs). FAMEs were purified by elution with dichloromethane over SiO_2 columns (~2 g). 5α androstane and hexamethylbenzene was used for quantification of the compounds on an Agilent Technologies 7890A gas chromatograph (GC) equipped with a VF1 column (30 m, 0.25 mm i.d., 0.25 μm film thickness) and a flame ionization detector (FID). Compound-specific δ^2H values of the long-chain *n*-alkanes and FAMEs were determined based on at least triplicate analyses on a gas chromatograph-pyrolysis-isotope ratio mass spectrometer (GC-pyrolysis-IRMS, Delta V, ThermoFisher Scientific, Bremen, Germany). The A4 standard mixture (provided by Arndt Schimmelmann, Indiana University, USA) was run three times per sequence at three different concentrations. All results are reported after normalization using multi-linear regression (Paul et al., 2007) and simple mass-balance correction of the FAMEs for the isotopic composition of the methanol used for derivatisation. Long-term precision of the analyses was monitored using a laboratory standard (oak, *n*-C_{29}). The standard was analyzed in every sequence and yielded a mean value of -147.2‰ with a standard deviation of ± 1.7 ‰ across all sequences run for this study.

149 **2.3. Modeling of leaf water ^{2}H enrichment**

150 The empirical data analyses were combined with mechanistic model simulations of $\delta^2H_{leaf\ water}$
151 in order to better detect and evaluate how the dominant climate variables (air temperature and
152 relative air humidity) influence ^{2}H enrichment in lipids. The ^{2}H enrichment of leaf water due
153 to evapotranspiration can be predicted by using mechanistic models originally developed for
154 isotope fractionation processes associated with evaporation from water surfaces by Craig and
155 Gordon (1965). These models were adapted for plants by Dongmann et al. (1974) and
156 subsequently by Flanagan et al. (1991) and Farquhar and Lloyd (1993). Evaporative ^{2}H
157 enrichment of the leaf water (Δ^2H_e) at the evaporative surface in the mesophyll is given by the
158 equation:

159 $$\Delta^2 H_e = \varepsilon^+ + \varepsilon_k + \left(\Delta^2 H_{WV} - \varepsilon_k\right)\frac{e_a}{e_i}, \qquad \text{(Eqn. 1)}$$

160 where ε^+ is the equilibrium fractionation between liquid water and vapor at the air-water
161 interfaces, ε_k is the kinetic fractionation during water vapor diffusion from leaf intercellular air
162 space to the atmosphere, Δ^2H_{WV} is the isotopic difference of the water vapor and the source
163 water, and e_a/e_i is the ratio of ambient to intercellular vapor pressure (Farquhar and Lloyd,
164 1993). This basic calculation was modified by including a Péclet effect that accounts for
165 opposing fluxes of source water entering the leaf through the transpiration flow and the back-
166 diffusion of isotopically enriched water from the sites of evaporation (Farquhar and Lloyd,
167 1993):

168 $$\Delta^2 H_{leafwater} = \frac{\Delta^2 H_e\left(1 - e^{-\wp}\right)}{EL/CD}. \qquad \text{(Eqn. 2)}$$

169 The quotient of EL/CD represents the Péclet number ($\wp$) where E is the transpiration rate, L
170 is the effective path length, C is the molar concentration of water and D is the diffusivity of
171 $^1H^2HO$. The model approach we used followed that of Kahmen et al. (2011b), where the
172 Péclet-modified Craig Gordon model is reduced to three input variables: air temperature,

atmospheric vapour pressure and source water δ^2H. This simplified model is based on the assumption that throughout the season leaf temperature equals air temperature and that atmospheric vapor δ^2H is generally in equilibrium with source water δ^2H (Kahmen et al. 2011b). Transpiration rates are estimated using relative humidity and air temperature (retrieved from GeoINTA, 2012) and assuming a mean stomatal conductance of 0.15 mol/m^2/s. Based on reports for a large number of species in the literature (Kahmen et al., 2008; Kahmen et al., 2009; Song et al., 2013), we used an average value of 20 mm for L and kept it constant across the transect. For our simulation of leaf water δ^2H values we obtained the model input variables air temperature, atmospheric vapor pressure and source water δ^2H from GeoINTA (2012) and Bowen (2012), respectively.

The isotopic composition of the leaf water can be estimated according to Eqn. 3:

$$\delta^2H_{leaf\ water} = \Delta^2H_{leaf\ water} + \delta^2H_{SW} \quad \text{(Eqn.3)},$$

where $\Delta^2H_{leaf\ water}$ is the bulk leaf water evaporative enrichment and δ^2H_{SW} is the hydrogen isotope ratio of source/xylem water.

2.4. Conceptual model for a coupled $\delta^{18}O$-δ^2H biomarker approach

The conceptual coupled $\delta^2H_{n\text{-alkane}}$-$\delta^{18}O_{sugar}$ model was introduced previously by Zech M. et al. (2013). In brief, it is based on the following fundamentals. Precipitation word-wide typically plots along/close to the so-called global meteoric water line (GMWL, $\delta^2H = 8 \times \delta^{18}O + 10$) in a $\delta^{18}O$-δ^2H diagram (Dansgaard, 1964) (Fig. 5). Due to fractionation processes, evaporation/transpiration causes water vapour to be isotopically depleted in ^{18}O and ^2H, whereas residual (leaf) water (δ^2H/$\delta^{18}O_{leaf\ water}$) is isotopically enriched. In a $\delta^{18}O$-δ^2H diagram, leaf water therefore does not plot on the GMWL but on an evaporation line (EL). The distance of leaf water to the Global Meteoric Water Line (GMWL) can be described as

199 deuterium excess (d = δ^2H - 8·δ^{18}O). Using a Craig-Gordon model adapted by Gat and
200 Bowser (1991), the d-excess of leaf water can be used to calculate RH values normalized to
201 the temperature of leaf-water (Zech et al., 2013):

202 $$RH = 1 - \frac{\Delta d}{\left(\varepsilon_2^* - 8 \cdot \varepsilon_{18}^* + C_k^2 - 8 \cdot C_k^{18}\right)} \quad \text{(Eqn. 4)}$$

203 where Δd represents the difference in d-excess between leaf-water and source water.
204 According to Merlivat (1978), experimentally determined kinetic isotope fractionation equals
205 25.1 ‰ and 28.5 ‰ for C_k^2 and C_k^{18}, respectively, considering that these are the maximum
206 values of kinetic fractionation during molecular diffusion of water through stagnant air.
207 Equilibrium isotope enrichments ε_2^* and ε_{18}^* as functions of temperature can be calculated
208 using empirical equations of Horita and Wesolowski (1994). Hence, provided that *n*-alkanes
209 and sugars in plants and soils reflect (albeit with a constant offset caused by biosynthetic
210 fractionation) the isotopic composition of leaf water, a coupled $\delta^2H_{n\text{-alkane}}$-$\delta^{18}O_{sugar}$ approach
211 allows reconstructing RH values. The biomarker-based reconstructed $\delta^2H/\delta^{18}O_{leaf\ water}$ values
212 allow furthermore reconstructing the isotopic composition of plant source water, which can be
213 considered in an approximation to reflect $\delta^2H/\delta^{18}O_{prec}$ (illustrated as intercepts of the
214 individual ELs with the GMWL in Fig. 5). Assuming a slope of ~2.82 seems reasonable both
215 based on model considerations and based on field observations and laboratory experiments
216 (Allison et al., 1985; Walker and Brunel, 1990; Bariac et al., 1994). For further details on
217 modelling coupled δ^{18}O-δ^2H biomarker results the reader is referred to Zech M. et al. (2013).
218
219 **3. Results and Discussion**
220
221 **3.1. Comparison of $\delta^2H_{n\text{-alkanes}}$ and $\delta^2H_{fatty\ acids}$**
222 The C_{29} and C_{31} *n*-alkane homologues were sufficiently abundant in all samples to be
223 measured for their hydrogen isotopic composition. The δ^2H values range from -155 to -222 ‰

and reveal a similar trend between *n*-C_{29} and *n*-C_{31} along the investigated transect (Table 1 and Fig. 2). While the northern and middle part of the transect is characterized by relatively high δ^2H values (~ -160 ‰), the southern part of the transect is characterized by considerably more negative δ^2H values (~ -210 ‰).

The δ^2H values of the fatty acids *n*-C_{22}, *n*-C_{24}, *n*-C_{26}, *n*-C_{28} and *n*-C_{30} range from -128 to -225 ‰ (Table 1 and Fig. 2). In general, there is a good overall agreement between the *n*-alkanes and the fatty acids ($R=0.96$, $p<0.001$, $n=20$; for the weighted means), both showing more negative δ^2H values in the south than in the northern and middle portions of the transect (Table 1, Fig. 2). Interestingly, the longer homologues *n*-C_{28} and *n*-C_{30} are systematically enriched by 3 ‰ to 43 ‰ compared to the *n*-alkanes. The same was observed by Chikaraishi and Naraoka (2007), reporting on *n*-alkanes being depleted in ^{2}H relative to the corresponding *n*-alkanoic acid. Reasons for this trend remain vague at this point, but may be relate to metabolic pathways, seasonal differences in homologue production, or differences in homologue sources. Roots, for example, have also been suggested as a source of long-chain *n*-fatty acids (Bull et al., 2000). Shorter homologues, have been suggested to be not only plant-derived, but also of bacterial origin (Matsumoto et al., 2007; Bianchi and Canuel, 2011). Similarly, soil microbial overprinting of long chain *n*-alkanes and fatty acids cannot be excluded (Nguyen Tu et al., 2011; Zech M. et al., 2011a). By contrast, there is strong evidence suggesting that *n*-alkanes are not produced by plants in significant amounts (Gamarra and Kahmen, 2015) and not significantly introduced into soils/subsoils by roots (Häggi et al., 2014).

The consistent δ^2H pattern revealed by the *n*-alkanes and fatty acids along the north-south climate transect does not solely reflect the δ^2H isotopic composition of precipitation. Especially in the middle part of the transect, δ^2H of the lipid biomarkers shows a pronounced offset (Fig. 3). Given that *n*-alkanes are considered to primarily reflect leaf signals and are

most widely applied in paleoclimate and paleohydrological studies, we will principally refer to δ^2H of long chain *n*-alkanes in further discussion and calculations.

3.2. Evapotranspirative ^{2}H enrichment of leaf water

Assuming a constant biosynthetic fractionation of -160 ‰ for the *n*-alkane and fatty acids biosynthesis in plants (Sessions et al., 1999; Sachse et al., 2006), we estimated the isotopic composition of leaf water using our *n*-alkane and fatty acids δ^2H values along the transect/gradient (Fig. 3). Note that an average biosynthetic fractionation factor of ~-200 ‰ was reported by Sessions et al. (1999) for short- and mid-chained fatty acids synthesized mostly by unicellular/multicellular marine algae. By contrast, there are hardly any biosynthetic fractionation factors reported for long-chained fatty acids of higher plants. Given that our δ^2H *n*-alkanes and fatty acids values are very similar, using a biosynthetic fractionation factor of -160 ‰ for both lipids seems appropriate.

Estimated leaf water δ^2H values suggest a pronounced ^{2}H enrichment of leaf water compared to precipitation (up to +62 ‰). This finding highlights the role of aridity for evapotranspiration and isotopic enrichment of leaf waxes, in good agreement with prior studies (Sachse et al., 2006; Feakins and Sessions, 2010; Douglas et al., 2012; Kahmen et al., 2013a).

Figure 4 illustrates the overall good agreement between $\delta^2H_{leaf\ water}$ values inferred from the measured *n*-alkanes and fatty acids, and $\delta^2H_{leaf\ water}$ values calculated using the Peclet-modified Craig-Gordon model. The correlations are highly significant ($r=0.88$, $p<0.001$, $n=20$, for *n*-alkanes and $r=0.93$, $p<0.001$, $n=20$ for fatty acids), suggesting that the model correctly implements the most relevant processes related to evapotranspirative enrichment of leaf water. While predicting the overall trend in leaf water δ^2H along the transect with reasonable accuracy, the model does not capture site-to-site excursions in the *n*-alkane-derived leaf water δ^2H values from this overall trend. As such, additional influences that are

not captured by the model, such as possible evaporative ^{2}H enrichment of soil water (see e.g. Dubbert et al., 2013), could explain the underestimation of the modeled $\delta^{2}H_{leaf\ water}$ values in the middle part of the transect (Fig. 4). In contrast, the model might overestimate $\delta^{2}H_{leaf\ water}$ in the southern part of the transect. The corresponding ecosystem, the Patagonian Steppe, is a grassland, whereas the middle part of the transect is dominated by shrubland. Grass-derived lipids have been shown to be less strongly affected by evaporative leaf water ^{2}H enrichment than those of trees or shrubs (McInerney et al., 2011; Yang et al., 2011; Sachse et al., 2012; Kahmen et al., 2013b), and hence the overestimation of the model may be due to plant species effects (Pedentchouk et al., 2008; Douglas et al., 2012). The more pronounced offsets in Patagonia could additionally be attributed to a seasonality effect. The growing season in Patagonia is not year-round but mainly in spring.

In order to assess the sensitivity of the model to the input parameters, we varied vapor pressure of air by +/- 5 hPa and mean annual temperature by +/- 5°C. Changing e_a in eq. (1) by ± 5 hPa corresponds to changes of RH from ca. 94% to 46% at the beginning of the transect and 89% to 15% at the end of the transect While changes in temperature have only negligible effects on the modeled $\delta^{2}H$ isotopic composition of leaf water, changes in RH yield difference in $\delta^{2}H_{leaf\ water}$ of up to ~30 ‰ (Fig. 4). Different climatic conditions during the spring growing season in Patagonia could thus explain the overestimation of the evapotranspirative enrichment in the model.

Evapotranspirative enrichment of leaf water has also been observed in $\delta^{18}O$ values of hemicellulose-derived arabinose, fucose and xylose analysed in topsoils along the investigated transect (Tuthorn et al., 2014). Model sensitivity tests of ^{18}O enrichment of leaf water using PMCG model corroborate the observations presented here that air humidity is the key factor defining the $^{18}O/^{2}H$ enrichment of leaf water.

3.3. Coupling of the $\delta^{2}H_{n\text{-alkane}}$ and $\delta^{18}O_{sugar}$ biomarker results

301 The conceptual model for the coupled $\delta^2H_{n\text{-alkan}}$-$\delta^{18}O_{sugar}$ biomarker approach is illustrated in
302 Fig. 5. The model is based on the assumption that the investigated *n*-alkane and hemicellulose
303 biomarkers are primarily leaf-derived and reflect the isotopic composition of leaf water. With
304 regard to the topsoil transect investigated here, this assumption is reasonable and supported by
305 leaf water modeling (for δ^2H in Section 3.2, and for $\delta^{18}O$ see Tuthorn et al., 2014).
306 Accordingly, biomarker-based 'reconstructed' $\delta^2H/\delta^{18}O_{leaf\ water}$ values can be calculated from
307 the biomarkers by applying biosynthetic fractionation factors ε_{bio}. For our reconstructions we
308 applied ε_{bio} factors of -160 ‰ (Sessions et al., 1999; Sachse et al., 2006) and +27 ‰
309 (Sternberg et al., 1986; Yakir and DeNiro, 1990; Schmidt et al., 2001; Cernusak et al., 2003;
310 Gessler et al., 2009) for δ^2H and $\delta^{18}O$, respectively (Fig. 5).
311
312 **3.3.1. Reconstructed RH values along the climate transect and comparison with actual**
313 **RH values**
314 The reconstructed d-excess values of leaf water along the investigated transect range from -67
315 to -178 ‰ and reveal a systematic trend towards more negative values in the south (Fig. 6).
316 The reconstructed RH values calculated using the leaf water d-excess values according to the
317 above-described coupled $\delta^2H_{n\text{-alkane}}$ - $\delta^{18}O_{sugar}$ approach range from 16 to 65 %, with one
318 extremely low value of 5 % (Fig. 6). Reconstructed RH values follow the systematic d-excess
319 trend and correlate significantly ($r=0.79$, $p<0.001$, $n=20$) with the actual mean annual RH
320 values retrieved from GeoINTA (2012) for all investigated sites.
321 However, as depicted by Fig. 6, the reconstructed RH values systematically underestimate the
322 actual mean annual RH values. This is especially pronounced for the three southernmost
323 locations (18-20) and may be attributed to several causes. First, the applied model calculations
324 do not account for evaporative enrichment of soil water. In the $\delta^{18}O$-δ^2H diagram, the soil
325 water enrichment shifts the source water (simplified to 'reconstructed precipitation' in Fig. 5
326 and our model) along the evaporation line and thus leads to too negative d-excess values and

an underestimation of RH. Second, given that leaf waxes are considered to be formed mostly during early stages of leaf ontogeny (Kolattukudy, 1970; Riederer & Markstaedter, 1996; Kahmen et al., 2011a; Tipple et al., 2013) they may not necessarily reflect the mean annual isotopic composition of precipitation in regions with pronounced seasonality, but rather the isotopic composition of precipitation during the growing season. Furthermore, mean annual RH values likely overestimate the RH values actually seen by leaves being photosynthetically active. Indeed when comparing the biomarker-based 'reconstructed' RH values with mean summer daytime RH values (available for 6 stations along the investigated transect from www.ncdc.noaa.gov), satisfactory agreement between 'reconstructed' and actual RH values is obtained, with the exception of the southern portion of the transect (Fig. 6). Third, the $\delta^{18}O$ biosynthetic fractionation factor of ~+27 ‰, which has been reported for newly assimilated sugars and cellulose, underestimates in our opinion the actual fractionation factor of hemicelluloses (Tuthorn et al., 2014; Zech M. et al., 2014a). This results in reconstructed leaf water values plotting too far to the right in the $\delta^{18}O$-$\delta^{2}H$ diagram (Fig. 5) and in turn to the observed underestimated RH values (Fig. 6). We argue with the loss of a relatively ^{18}O-depleted oxygen atom attached to C-6 during pentose biosynthesis (C-6 decarboxylation; Altermatt and Neish, 1956; Harper and Bar-Peled, 2002; Burget et al., 2003) and point to a recent study of Waterhouse et al. (2013) who have determined the position specific $\delta^{18}O$ values in cellulose. Further experimental studies as suggested and encouraged by Sternberg (2014) and Zech M. et al. (2014b) are urgently needed to ascertain an improved biosynthetic fractionation factor for hemicellulose-derived sugars.

3.3.2. Comparison of reconstructed and actual $\delta^{2}H_{prec}$ and $\delta^{18}O_{prec}$ values

Values of $\delta^{18}O_{prec}$ and $\delta^{2}H_{prec}$ reconstructed as the intercepts of the individual evaporation lines (EL) with the GMWL in the $\delta^{18}O$-$\delta^{2}H$ diagram (Fig. 5) range from -7 to -22 ‰ and from -47 to -166 ‰, respectively. They correlate highly significantly (Fig. 7; r=0.90, p<0.001,

353 n=20, and r=0.88, p<0.001, n=20 for $\delta^{18}O_{prec}$ and $\delta^{2}H_{prec}$, respectively) with the 'actual'[1]
354 $\delta^{2}H_{prec}$ and $\delta^{18}O_{prec}$ values as derived from Bowen (2012). While the reconstructed $\delta^{18}O_{prec}$
355 and $\delta^{2}H_{prec}$ values, like the reconstructed RH values, generally validate our conceptual model,
356 they appear to systematically underestimate the actual $\delta^{18}O$ and $\delta^{2}H$ values of the
357 precipitation water (Fig. 7).
358 The uncertainties discussed above for the observed offset of 'reconstructed' versus actual RH
359 values can also affect the accuracy of reconstructed $\delta^{18}O_{prec}$ and $\delta^{2}H_{prec}$ values. Hence, the
360 'actual' $\delta^{2}H/\delta^{18}O_{prec}$ values used for our comparison with the biomarker-based 'reconstructed'
361 values can be assumed to be one of the possible sources of uncertainty . While Bowen (2012)
362 reported a confidence interval (95%) ranging from 0.2‰ to 1.2‰, and from 2‰ to 11‰ for
363 $\delta^{2}H_{prec}$ and $\delta^{18}O_{prec}$, respectively, future climate transect studies will be ideally carried out
364 with actual precipitation being sampled for $\delta^{2}H/\delta^{18}O$ analyses. Moreover, we would like to
365 emphasize also here the very likely influence of seasonality. As reported for sugar biomarkers
366 (Tuthorn et al., 2014), we suggest that also leaf waxes mainly reflect the humidity and the
367 isotopic composition of spring and summer precipitation rather than mean annual values.
368

369 **5. Conclusions**

370

371 The hydrogen isotopic composition of leaf wax *n*-alkanes and *n*-alkanoic (fatty) acids
372 extracted from topsoils along a transect in Argentina varies significantly, with $\delta^{2}H$ values
373 ranging from -155 to -222 ‰ and -128 to -225 ‰, respectively. These $\delta^{2}H$ values broadly
374 parallel variations in the hydrogen isotopic composition of precipitation, but are modulated by
375 evaporative ^{2}H enrichment of leaf water. A mechanistic leaf water model correctly simulates

[1] Please note that we chose here the term ‚actual' for reasons of simplification in order to make the difference to the biomarker-based 'reconstructed' $\delta^{18}O_{prec}$ and $\delta^{2}H_{prec}$ values. Indeed, both the 'reconstructed' and the 'actual' values are derived from modelling, namely from our conceptual $\delta^{2}H_{n\text{-alkane}}$-$\delta^{18}O_{sugar}$ model and from Bowen's (2012) online isotopes in precipitation calculator.

the overall trends. Sensitivity tests show that relative humidity exerts a much stronger influence on evaporative enrichment than temperature.

Based on the premise that *n*-alkanes and hemicellulose biomarkers are primarily leaf-derived, we reconstruct $\delta^2H_{leaf\ water}$ and $\delta^{18}O_{leaf\ water}$, respectively, which in turn allows assessment of the d-excess of leaf water. The large calculated range in d-excess along the transect (-67 to -178 ‰) can be used to calculate biomarker-based 'reconstructed' RH values. 'Reconstructed' RH values correlate significantly with actual mean annual RH values along the transect. Despite this overall correlation, 'reconstructed' RH values systematically underestimate actual mean annual RH values. However, this discrepancy is largely reduced when 'reconstructed' RH values are compared with actual mean summer daytime RH values. Similarly, biomarker-based 'reconstructed' $\delta^{18}O_{prec}$ and δ^2H_{prec} values correlate highly significantly with 'actual' $\delta^{18}O_{prec}$ and δ^2H_{prec} values, but reveal systematic offsets, too.

We conclude that compared to single $\delta^2H_{n\text{-alkane}}$ or $\delta^{18}O_{sugar}$ records, the proposed coupled $\delta^2H_{n\text{-alkane}}$-$\delta^{18}O_{sugar}$ approach will allow more robust $\delta^2H/\delta^{18}O_{prec}$ reconstructions and additionally the reconstruction of mean summer daytime RH changes/history using d-excess of leaf water as proxy in future paleoclimate studies. However, further studies are needed to ascertain an improved biosynthetic fractionation factor for hemicellulose-derived sugars. Also, in the light of strong diurnal variations of δ^2H and $\delta^{18}O$ of leaf water, it would be important to determine which portion of this diurnal signal is actually incorporated in the *n*-alkanes and sugars being synthesized in the leaves.

Acknowledgements

We kindly thank Prof. B. Huwe (University Bayreuth) and Prof. L. Zöller (University Bayreuth) for logistic support. This study was partly financed by the SIBAE COST Action ES0806, the German Research Foundation (DFG Oe516/2-1 and ZE 844/1-2), the Swiss National Science Foundation (SNF Ambizione PZ00P2_131670) and the statutory funds of

the AGH University of Science and Technology. This publication was funded by the German Research Foundation (DFG) and the University of Bayreuth in the funding programme Open Access Publishing. We kindly thank Prof. Y Kuzyakov for the editorial handling of our MS, as well as an anonymous referee and Marie Galeron for constructive comments on our MS.

References

Allison, G.B., Gat, J.R., Leaney, F.W.J., 1985. The relationship between deuterium and oxygen-18 delta values in leaf water. Chemical Geology 58, 145-156.

Altermatt, H.A., Neish, A.C., 1956. The biosynthesis of cell wall carbohydrates: III. further studies on formation of cellulose and xylan from labeled monosaccharides in wheat plants. Canadian Journal of Biochemistry and Physiology 34, 405-413.

Araguas-Araguas, L., Froehlich, K., Rozanski, K., 2000. Deuterium and oxygen-18 isotope composition of precipitation and atmospheric moisture. Hydrological Processes 14, 1341-1355.

Bariac, T., Gonzales-Dunia, J., Katerji, N., Bethenod, O., Bertolini, J.M., Mariotti, A., 1994. Spatial variation of the isotopic composition of water (^{18}O, ^{2}H) in the soil-plant-atmosphere system. Chemical Geology 115, 317-333.

Bianchi, T., Canuel, E.A., 2011. Chemical Biomarkers in Aquatic Ecosystems. Princeton University Press, Princeton.

Bowen, G.J., 2012 The Online Isotopes in Precipitation Calculator, version 2.2. http://www.waterisotopes.org.

Bull, I.D., Nott, C.J., van Bergen, P.F., Poulton, P.R., Evershed, R.P., 2000. Organic geochemical studies of soils from the Rothamsted classical experiments - VI. The occurrence and source of organic acids in an experimental grassland soil. Soil Biology and Biochemistry 32, 1367-1376.

Burget, E., Verma, R., Mølhøj, M., Reiter, W., 2003. The biosynthesis of L-arabinose in plants: molecular cloning and characterization of a golgi-localized UDP-D-xylose 4-epimerase encoded by the MUR4 gene of arabidopsis. The Plant Cell 15, 523-531.

Burgos, J.J., Vidal, A.L., 1951. Los climas de la República Argentina, segun la nueva clasificación de Thornthwaite. Meteoros 1, 1-32.

Cernusak, L.A., Wong, S.C., Farquhar, G.D., 2003. Oxygen isotope composition of phloem sap in relation to leaf water in *Ricinus communis*. Functional Plant Biology 30, 1059-1070.

Chikaraishi, Y., Naraoka H., 2007. $\delta^{13}C$ and δD relationships among three n-alkyl compound classes (n-alkanoic acid, n-alkane and n-alkanol) of terrestrial higher plants. Organic Geochemistry 38, 198-215.

Craig, H., Gordon, L.I., 1965 Deuterium and oxygene-18 variations in the ocean and the marine atmosphere. In: Conference on Stable Isotopes in Oceanographic Studies and Paleotemperatures (Ed. by E. Tongiorgi), pp. 9-130, Spoleto, Italy.

Dansgaard W., 1964. Stable isotopes in precipitation. Tellus 16, 436-468.

Dongmann, G., Nürnberg, H.W., Förstel, H., Wagener, K., 1974. On the enrichment of $H_2{}^{18}O$ in the leaves of transpiring plants. Radiation and Environmental Biophysics 11, 41-52.

Douglas, P.M.J., Pagani, M., Brenner, M., Hodell, D.A., Curtis, J.H., 2012. Aridity and vegetation composition are important determinants of leaf-wax δD values in southeastern Mexico and Central America. Geochimica et Cosmochimica Acta 97, 24-45.

Dubbert, M., Cuntz, M., Piayda, A., Maguás, Werner, C., 2013. Partitioning evapotranspiration - Testing the Craig and Gordon model with field measurements of oxygen isotope ratios of evaporative fluxes. Journal of Hydrology, 496, 142-153

Eglinton, G., Hamilton, R.J., 1967. Leaf Epicuticular Waxes. Science 156, 1322-1335.

Eglinton, T.I., Eglinton, G., 2008. Molecular proxies for paleoclimatology. Earth and Planetary Science Letters 275, 1-16.
Ehleringer, J.R., Dawson, T.E., 1992. Water uptake by plants: perspectives from stable isotope composition. Plant, Cell & Environment 15, 1073-1082.
Farquhar, G.D., Cernusak, L.A., Barnes, B., 2007. Heavy Water Fractionation during Transpiration. Plant Physiology 143, 11-18.
Farquhar, G.D., Lloyd, J., 1993 Carbon and oxygene isotope effects in the exchange of carbon dioxide between terrestrial plants and the atmosphere, In: J.R. Ehleringer, A.E. Hall, G.D. Farquhar (Eds.), Stable isotopes and plant carbon-water relations. Academic Press, Inc., San Diego, pp. 47-70.
Feakins, S.J., Sessions, A.L., 2010. Controls on the D/H ratios of plant leaf waxes in an arid ecosystem. Geochimica et Cosmochimica Acta 74, 2128-2141.
Fernández, O.A., Busso, C.A., 1997 Arid and semi-arid rangelands: two thirds of Argentina, pp. 41-60. RALA Report 200.
Flanagan, L.B., Comstock, J.P., Ehleringer, J.R., 1991. Comparison of modeled and observed environmental influences on the stable oxygen and hydrogen isotope composition of leaf water in *Phaseolus vulgaris* L. Plant Physiology 96, 588-596.
Gamarra, B., Kahmen, A., 2015. Concentrations and d2H values of cuticular n-alkanes vary significantly among plant organs, species and habitats in grasses from alpine and a temperated European grassland. Oecologia DOI 10.1007/s00442-015-3278-6.
Gat, J.R., 1996. Oxygen and Hydrogen Isotopes in the Hydrologic Cycle. Annual Review of Earth and Planetary Sciences 24, 225-262.
Gat, J.R., Bowser, C., 1991 The heavy isotope enrichment of water in coupled evaporative systems, In: H.P. Taylor, J.R. O'Neil, I.R. Kaplan (Eds.), Stable Isotope Geochemistry: A Tribute to Samuel Epstein. The Geochemical Society, Lancester, pp. 159-168.
GeoINTA, 2012 Instituto Nacional de Technologia Agropecuaria Visualizador Integrado. Available online at: http://geointa.inta.gov.ar/visor/ . Accessed 01.08.2012.
Gessler, A., Brandes, E., Buchmann, N., Helle, G., Rennenberg, H., Barnard, R.L., 2009. Tracing carbon and oxygen isotope signals from newly assimilated sugars in the leaves to the tree-ring archive. Plant, Cell & Environment 32, 780-795.
Greule, M., Hänsel, C., Bauermann, U., Mosandl, A., 2008. Feed additives: authenticity assessment using multicomponent-/multielement-isotope ratio mass spectrometry. European Food Research and Technology 227, 767-776.
Häggi, C., Zech, R., McIntyre, C., Zech, M. and Eglinton, T., 2014. On the stratigraphic integrity of leaf-wax biomarkers in loess paleosol. Biogeosciences 11, 2455-2463.
Harper, A., Bar-Peled, M., 2002. Biosynthesis of UDP-xylose. Cloning and characterization of a novel Arabidopsis gene family, UXS, encoding soluble and putative membrane-bound UDP-glucuronic acid decarboxylase isoforms. Plant Physiology 130, 2188-2198.
Hener, U., Brand, W.A., Hilkert, A.W., Juchelka, D., Mosandl, A., Podebrad, F., 1998. Simultaneous on-line analysis of 18O/16O and 13C/12C ratios of organic compounds using GC-pyrolysis-IRMS. Zeitschrift für Lebensmitteluntersuchung und -Forschung A 206, 230-232.
Horita, J., Wesolowski, D.J., 1994. Liquid-vapor fractionation of oxygen and hydrogen isotopes of water from the freezing to the critical temperature. Geochimica et Cosmochimica Acta 58, 3425-3437.
Huang, Y., Shuman, B., Wang, Y., Webb, T., 2004. Hydrogen isotope ratios of individual lipids in lake sediments as novel tracers of climatic and environmental change: a surface sediment test. Journal of Paleolimnology 31, 363-375.
Juchelka, D., Beck, T., Hener, U., Dettmar, F., Mosandl, A., 1998. Multidimensional Gas Chromatography Coupled On-Line with Isotope Ratio Mass Spectrometry (MDGC-IRMS): Progress in the Analytical Authentication of Genuine Flavor Components. Journal of High Resolution Chromatography 21, 145-151.
Jung, J., Puff, B., Eberts, T., Hener, U., Mosandl, A., 2007. Reductive ester cleavage of acyl glycerides-GC-C/P-IRMS measurements of glycerol and fatty alcohols. European Food Research and Technology 225, 191-197.
Jung, J., Sewenig, S., Hener, U., Mosandl, A., 2005. Comprehensive authenticity assessment of lavender oils using multielement/multicomponent isotope ratio mass spectrometry analysis

and enantioselective multidimensional gas chromatography-mass spectrometry. European Food Research and Technology 220, 232-237.
Kahmen, A., Dawson, T.E., Vieth, A., Sachse, D., 2011a. Leaf wax *n*-alkane δD values are determined early in the ontogeny of *Populus trichocarpa* leaves when grown under controlled environmental conditions. Plant, Cell & Environment 34, 1639-1651.
Kahmen A., Sachse D., Arndt S.K., Tu K.P., Farrington H., Vitousek P.M., and Dawson T.E., 2011b. Cellulose $\delta^{18}O$ is an index of leaf-to-air vapor pressure difference (VPD) in tropical plants. Proceedings of the National Academy of Sciences 108, 1981-1986.
Kahmen, A., Hoffmann, B., Schefuss, E., Arndt, S.K., Cernusak, L.A., West, J.B., Sachse, D., 2013a. Leaf water deuterium enrichment shapes leaf wax *n*-alkane δD values of angiosperm plants II: Observational evidence and global implications. Geochimica et Cosmochimica Acta 111, 50-63.
Kahmen, A., Schefuß, E., Sachse, D., 2013b. Leaf water deuterium enrichment shapes leaf wax *n*-alkane δD values of angiosperm plants I: Experimental evidence and mechanistic insights. Geochimica et Cosmochimica Acta 111, 39-49.
Kahmen, A., Simonin K., Tu, K., Goldsmith, G.R., Dawson, T.E., 2009. The influence of species and growing conditions on the 18-O enrichment of leaf water and its impact on 'effective path length'. New Phytologist, 184, 619-630.
Kahmen, A., Simonin, K., Tu, K.P., Merchant, A., Callister, A., Siegwolf, R., Dawson, T.E., Arndt, S.K., 2008. Effects of environmental parameters, leaf physiological properties and leaf water relations on leaf water $\delta^{18}O$ enrichment in different Eucalyptus species. Plant, Cell & Environment 31, 738-751.
Kolattukudy, P., 1970. Cutin biosynthesis in *Vicia faba* leaves - effect of age. Plant Physiology 46, 759-760.
Le Houérou, H.N., 1996. Climate change, drought and desertification. Journal of Arid Environments 34, 133-185.
Matsumoto, K., Kawamura, K., Uchida, M., Shibata, Y., 2007. Radiocarbon content and stable carbon isotopic ratios of individual fatty acids in subsurface soils: Implication for selective microbial degradation and modification of soil organic matter. Geochemical Journal 41, 483-492.
McInerney, F.A., Helliker, B.R., Freeman, K.H., 2011. Hydrogen isotope ratios of leaf wax *n*-alkanes in grasses are insensitive to transpiration. Geochimica et Cosmochimica Acta 75, 541-554.
Merlivat, L., 1978. Molecular diffusivities of $H_2{}^{16}O$,$HD^{16}O$, and $H_2{}^{18}O$ in gases. The Journal of Chemical Physics 69, 2864-2871.
Nguyen Tu, T.T., Egasse, C.l., Zeller, B., Bardoux, G.r., Biron, P., Ponge, J.-F.o., David, B., Derenne, S., 2011. Early degradation of plant alkanes in soils: A litterbag experiment using 13C-labelled leaves. Soil Biology and Biochemistry 43, 2222-2228.
Pagani, M., Pedentchouk, N., Huber, M., Sluijs, A., Schouten, S., 2006. Arctic hydrology during global warming at the Paleocene/Eocene thermal maximum. Nature 442, 671-675.
Paruelo, J.M., Beltrán, A., Jobbágy, E., Sala, O.E., Golluscio, R.A., 1998. The climate of Patagonia: general patterns and controls on biotic processes. Ecologia Austral 8, 85-101.
Paul, D., Skrzypek, G., Fórizs, I., 2007. Normalization of measured stable isotopic compositions to isotope reference scales - a review. Rapid Communications in Mass Spectrometry 21, 3006-3014.
Pedentchouk, N., Sumner, W., Tipple, B., Pagani, M., 2008. delta C-13 and delta D compositions of *n*-alkanes from modern angiosperms and conifers: An experimental set up in central Washington State, USA. Organic Geochemistry 39, 1066-1071.
Rao, Z., Zhu, Z., Jia, G., Henderson, A.C.G., Xue, Q., Wang, S., 2009. Compound specific δD values of long chain *n*-alkanes derived from terrestrial higher plants are indicative of the δD of meteoric waters: Evidence from surface soils in eastern China. Organic Geochemistry 40, 922-930.
Riederer, M., Markstaedter, C., 1996 Cuticular waxes: a critical assessment of current knowledge, In: K.G. Kerstiens (Ed.), Plant Cuticules - An Integrated Functional Approach. BIOS Scientific Publishers, Oxford.
Rozanski, K., Araguas-Araguas, L., Gonfiantini, R., 1993. Isotopic patterns in modern global precipitation. In: P.K. Swart et al. (Editor), Climate Change in Continental Isotopic Records.

561 Geophysical Monograph 78, American Geophysical Union, Washington, DC 20009, USA, pp.
562 1-37.
563 Ruppenthal, M., Oelmann, Y., Francisco del Valle, H., Wilcke, W., 2015. Stable isotope ratios of
564 nonexchangeable hydrogen in organic matter of soils and plants along a 2100-km
565 climosequence in Argentina: New insights into soil organic matter sources and
566 transformations? Geochimica Et Cosmochimica Acta 152:54-71
567 Sachse, D., Billault, I., Bowen, G.J., Chikaraishi, Y., Dawson, T.E., Feakins, S.J., Freeman, K.H.,
568 Magill, C.R., McInerney, F.A., van der Meer, M.T.J., Polissar, P., Robins, R.J., Sachs, J.P.,
569 Schmidt, H.-L., Sessions, A.L., White, J.W.C., West, J.B., Kahmen, A., 2012. Molecular
570 Paleohydrology: Interpreting the Hydrogen-Isotopic Composition of Lipid Biomarkers from
571 Photosynthesizing Organisms. Annual Review of Earth and Planetary Sciences 40, 221-249.
572 Sachse, D., Radke, J., Gleixner, G., 2004. Hydrogen isotope ratios of recent lacustrine sedimentary *n*-
573 alkanes record modern climate variability. Geochimica et Cosmochimica Acta 68, 4877-4889.
574 Sachse, D., Radke, J., Gleixner, G., 2006. δD values of individual *n*-alkanes from terrestrial plants
575 along a climatic gradient - Implications for the sedimentary biomarker record. Organic
576 Geochemistry 37, 469-483.
577 Samuels, L., Kunst, L., Jetter, R., 2008. Sealing Plant Surfaces: Cuticular Wax Formation by
578 Epidermal Cells. Annual Review of Plant Biology 59, 683-707.
579 Sauer, P.E., Eglinton, T.I., Hayes, J.M., Schimmelmann, A., Sessions, A.L., 2001. Compound-specific
580 D/H ratios of lipid biomarkers from sediments as a proxy for environmental and climatic
581 conditions. Geochimica et Cosmochimica Acta 65, 213-222.
582 Schefuss, E., Schouten, S., Schneider, R.R., 2005. Climatic controls on central African hydrology
583 during the past 20,000 years. 437, 1003-1006.
584 Schmidt, H.-L., Werner, R.A., Rossmann, A., 2001. ^{18}O pattern and biosynthesis of natural plant
585 products. Phytochemistry 58, 9-32.
586 Sessions, A.L., Burgoyne, T.W., Schimmelmann, A., Hayes, J.M., 1999. Fractionation of hydrogen
587 isotopes in lipid biosynthesis. Organic Geochemistry 30, 1193-1200.
588 Smith, F.A., Freeman, K.H., 2006. Influence of physiology and climate on δD of leaf wax *n*-alkanes
589 from C3 and C4 grasses. Geochimica et Cosmochimica Acta 70, 1172-1187.
590 Song X., Barbour M.M., Farquhar G.D., Vann D.R., Helliker B.R.,2013. Transpiration rate relates to
591 within- and across-species variations in effective path length in a leaf water model of oxygene
592 isotope enrichment. Plant, Cell and Environment 36, 1338-1351.
593 Sternberg, L., DeNiro, M.J., Savidge, R.A., 1986. Oxygen isotope exchange between metabolites and
594 water during biochemical reactions leading to cellulose synthesis. Plant Physiology 82, 423-
595 427.
596 Sternberg, L., 2014. Comment on "Oxygen isotope ratios ($^{18}O/^{16}O$) of hemicellulose-derived sugar
597 biomarkers in plants, soils and sediments as paleoclimate proxy I: Insight from a climate
598 chamber experiment" by Zech et al. (2014). Geochim Cosmochim Acta 141, 677-679.
599 Tierney, J.E., Russel, J.M., Huang, Y., Sinninghe Damsté, J.S., Hopmans, E.C., Cohen, A.S., 2008.
600 Northern Hemisphere Controls on Tropical Southeast African Climate During the Past 60,000
601 Years. Science 322, 252-255.
602 Tipple, B.J., Berke, M.A., Doman, C.E., Khachaturyan, S., Ehleringer, J.R., 2013. Leaf-wax *n*-alkanes
603 record the plant-water environment at leaf flush. Proceedings of National Academy of Science
604 110, 2659-2664.
605 Tuthorn, M., Zech, M., Ruppenthal, M., Oelmann, Y., Kahmen, A., Valle, H.c.F.d., Wilcke, W.,
606 Glaser, B., 2014. Oxygen isotope ratios (18O/16O) of hemicellulose-derived sugar biomarkers
607 in plants, soils and sediments as paleoclimate proxy II: Insight from a climate transect study.
608 Geochimica et Cosmochimica Acta 126, 624-634.
609 Walker, C.D., Brunel, J.-P., 1990. Examining evapotranspiration in a semi-arid region using stable
610 isotopes of hydrogen and oxygen. Journal of Hydrology 118, 55-75.
611 Waterhouse, J.S., Cheng, S., Juchelka, D., Loader, N.J., McCarroll, D., Switsur, V.R., Gautam, L.,
612 2013. Position-specific measurement of oxygen isotope ratios in cellulose: Isotopic exchange
613 during heterotrophic cellulose synthesis. Geochimica et Cosmochimica Acta 112, 178-191.
614 Yakir, D., 1992. Variations in the natural abundance of oxygen-18 and deuterium in plant
615 carbohydrates. Plant, Cell & Environment 15, 1005-1020.

Yakir, D., DeNiro, M.J., 1990. Oxygen and hydrogen isotope fractionation during cellulose metabolism in *Lemna gibba* L. Plant Physiology 93, 325-332.

Yang, H., Liu, W., Leng, Q., Hren, M.T., Pagani, M., 2011. Variation in *n*-alkane δD values from terrestrial plants at high latitude: Implications for paleoclimate reconstruction. Organic Geochemistry 42, 283-288.

Zech, M., Glaser, B., 2009. Compound-specific $\delta^{18}O$ analyses of neutral sugars in soils using gas chromatography-pyrolysis-isotope ratio mass spectrometry: problems, possible solutions and a first application. Rapid Communications in Mass Spectrometry 23, 3522-3532.

Zech, M., Pedentchouk, N., Buggle, B., Leiber, K., Kalbitz, K., Markovic, S.B., Glaser, B., 2011a. Effect of leaf litter degradation and seasonality on D/H isotope ratios of *n*-alkane biomarkers. Geochimica et Cosmochimica Acta 75, 4917-4928.

Zech, M., Zech, R., Buggle, B., and Zöller, L., 2011b. Novel methodological approaches in loess research – interrogating biomarkers and compound-specific stable isotopes. Eiszeitalter & Gegenwart – Quaternary Science Journal 60 (1), 170-187.

Zech, M., Werner, R.A., Juchelka, D., Kalbitz, K., Buggle, B., Glaser, B., 2012. Absence of oxygen isotope fractionation/exchange of (hemi-) cellulose derived sugars during litter decomposition. Organic Geochemistry 42, 1470-1475.

Zech, M., Tuthorn, M., Detsch, F., Rozanski, K., Zech, R., Zoeller, L., Zech, W., Glaser, B., 2013. A 220 ka terrestrial $\delta^{18}O$ and deuterium excess biomarker record from an eolian permafrost paleosol sequence, NE-Siberia. Chemical Geology 360-361, 220-230.

Zech, M., Mayr, C., Tuthorn, M., Leiber-Sauheitl, K., Glaser, B., 2014a. Oxygen isotope ratios (18O/16O) of hemicellulose-derived sugar biomarkers in plants, soils and sediments as paleoclimate proxy I: Insight from a climate chamber experiment. Geochimica et Cosmochimica Acta 126, 614-623.

Zech, M., Mayr, C., Tuthorn, M., Leiber-Sauheitl, K. and Glaser, B., 2014b. Reply to the comment of Sternberg on "Zech et al. (2014) Oxygen isotope ratios ($^{18}O/^{16}O$) of hemicellulose-derived sugar biomarkers in plants, soils and sediments as paleoclimate proxy I: Insight from a climate chamber experiment". GCA 126, 614-623. Geochimica et Cosmochimica Acta 141, 680-682.

Zech, M., Zech, R., Rozanski, K., Gleixner, G. and Zech, W., 2015. Do *n*-alkane biomarkers in soils/sediments reflect the $\delta^{2}H$ isotopic composition of precipitation? A case study from Mt. Kilimanjaro and implications for paleoaltimetry and paleoclimate research. Isotope in Environmental and Health Studies, accepted.

Zech, R., Zech, M., Markovic, S., Hambach, U., Huang, Y., 2013. Humid glacials, arid interglacials? Critical thoughts on pedogenesis and paleoclimate based on multi-proxy analyses of the loess-paleosol sequence Crvenka, Northern Serbia. Palaeogeography, Palaeoclimatology, Palaeoecology 387, 165-175.

List of Tables and Figures

Table 1: δ^2H values of individual leaf wax *n*-alkanes and fatty acids. Measurements were carried out in at least triplicate (sd = standard deviation).

Fig. 1: Sampling locations along the investigated transect in Argentina. The colors illustrate the gradient in δ^2H_{prec}, and mean annual temperature and precipitation are shown below.

Fig. 2: Comparison of δ^2H results of individual leaf wax *n*-alkanes and *n*-alkanoic (fatty) acids along the investigated transect.

Fig. 3: Comparison of measured $\delta^2H_{n\text{-alkanes}}$ (weighted mean of *n*-C_{29} and *n*-C_{31}) and $\delta^2H_{fatty\ acids}$ (weighted mean of *n*-C_{22}, *n*-C_{24}, *n*-C_{26}, *n*-C_{28} and *n*-C_{30}) pattern with δ^2H_{prec} (Bowen, 2012) along the north-south climate transect (^{x}min and $^{+}$max representing annual minimum and maximum value at the sampling site). Additionally, assuming a biosynthetic fractionation of -160 ‰ for the *n*-alkane and fatty acid biosynthesis in plants the biomarker-based ‘reconstructed’ isotopic composition of leaf water is shown.

Fig. 4: Results of $\delta^2H_{leaf\ water}$ model simulations and comparison with biomarker-based ‘reconstructed’ (assuming a biosynthetic fractionation factor of -160 ‰) isotopic composition of leaf water based on *n*-alkanes and fatty acids, respectively. Sensitivity tests for $\delta^2H_{leaf\ water}$ are shown for changes in RH and air temperature for all 20 sites along the transect.

Fig. 5: δ^{18}O-δ^2H diagram illustrating the conceptual model of the coupled $\delta^2H_{n\text{-alkane}}$-$\delta^{18}O_{sugar}$ approach (modified after Zech M. et al., 2013a). $\delta^2H_{n\text{-alkane}}$ (mean of *n*-C_{29} and *n*-C_{31}) and $\delta^{18}O_{sugar}$ (mean of arabinose, fucose and xylose) results are used to reconstruct $\delta^2H/\delta^{18}O_{leaf\ water}$ by subtracting the biosynthetic fractionation factors. The deuterium excess ($d = \delta^2H - 8\cdot\delta^{18}O$) of leaf water serves as proxy for RH and $\delta^2H/\delta^{18}O_{prec}$ is

679 calculated as intersection of the individual evaporation lines (ELs, slope 2.82) with the
680 global meteoric water line (GMWL).

681 **Fig. 6:** Comparison of biomarker-based 'reconstructed' relative humidity (RH) values with
682 actual RH values (mean annual RH retrieved for all investigated sites from GeoINTA,
683 2012; summer daytime RH for six stations retrieved from www.ncds.noaa.gov).
684 Deuterium excess values were calculated using $\delta^{18}O_{leaf\ water}$ reconstructed from
685 terrestrial sugars (Tuthorn et al., 2014) and $\delta^{2}H_{leaf\ water}$ reconstructed from *n*-alkanes.

686 **Fig. 7:** Correlation of biomarker-based 'reconstructed' $\delta^{18}O_{prec}$ and $\delta^{2}H_{prec}$ values with
687 modern 'actual' $\delta^{18}O_{prec}$ and $\delta^{2}H_{prec}$ values (from Bowen, 2012).

Table 1: δ^2H values of individual leaf wax *n*-alkanes and fatty acids. Measurements were carried out in at least triplicate (sd = standard deviation).

	$\delta^2H_{n\text{-alkanes}}$				$\delta^2H_{fatty\ acids}$									
	C_{29}		C_{31}		C_{22}		C_{24}		C_{26}		C_{28}		C_{30}	
sampling locality	mean (‰)	sd	mean (‰)	sd	mean (‰)	sd	mean (‰)	sd	mean (‰)	sd	mean (‰)	sd	mean (‰)	sd
1	-157	2	-164	2	-155	1	-157	1	-151	1	-153	1	-153	2
2	-166	0	-166	1	-150	0	-155	1	-165	1	-163	1	-161	3
3	-175	1	-179	1	-162	0	-161	1	-165	1	-159	1	-155	0
4	-176	1	-176	1	-162	2	-163	1	-166	1	-165	1	-158	2
5	-178	1	-180	2	-164	0	-165	1	-168	2	-162	1	-159	1
6	-171	2	-172	0	-166	0	-165	2	-169	1	-161	1	-158	1
7	-179	0	-182	0	-170	0	-172	1	-177	0	-169	1	-157	0
8	-162	1	-167	1	-161	1	-161	1	-166	1	-161	1	-158	2
9	-173	1	-168	1	-163	1	-164	0	-168	1	-169	0	-156	1
10	-173	2	-170	2	-159	1	-167	1	-168	0	-159	1	-137	2
11	-170	2	-156	2	-158	0	-169	0	-167	2	-153	4	-147	4
12	-155	1	-176	0	-158	1	-168	1	-172	1	-148	1	-133	1
13	-157	2	-161	1	-158	1	-153	0	-140	1	-135	1	-128	1
14	-158	1	-166	0	-168	1	-183	0	-181	2	-160	2	-147	1
15	-194	2	-193	1	-194	0	-197	0	-191	1	-176	2	-168	2
16	-203	1	-211	1	-204	1	-198	0	-201	0	-193	0	-189	1
17	-218	1	-217	1	-219	1	-220	1	-217	0	-205	1	-204	1
18	-213	1	-202	4	-211	0	-203	1	-204	0	-196	0	-194	0
19	-222	1	-222	1	-220	0	-210	0	-225	1	-212	1	-204	1
20	-220	1	-212	1	-225	0	-221	1	-211	1	-193	3	-195	2

688

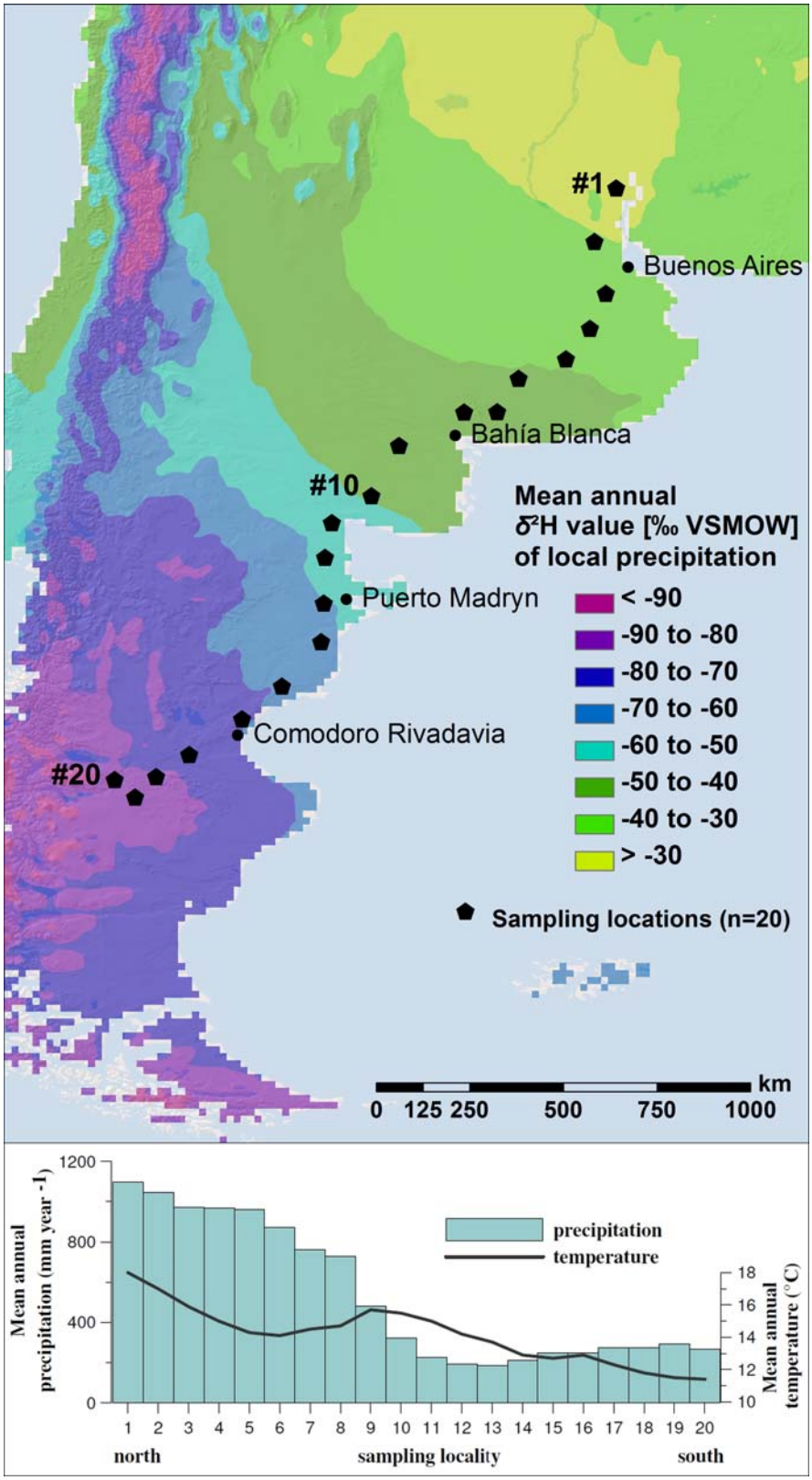

689

690 **Fig. 1**: Sampling locations along the investigated transect in Argentina. The colors illustrate
691 the gradient in δ^2H_{prec}, and mean annual temperature and precipitation are shown
692 below.

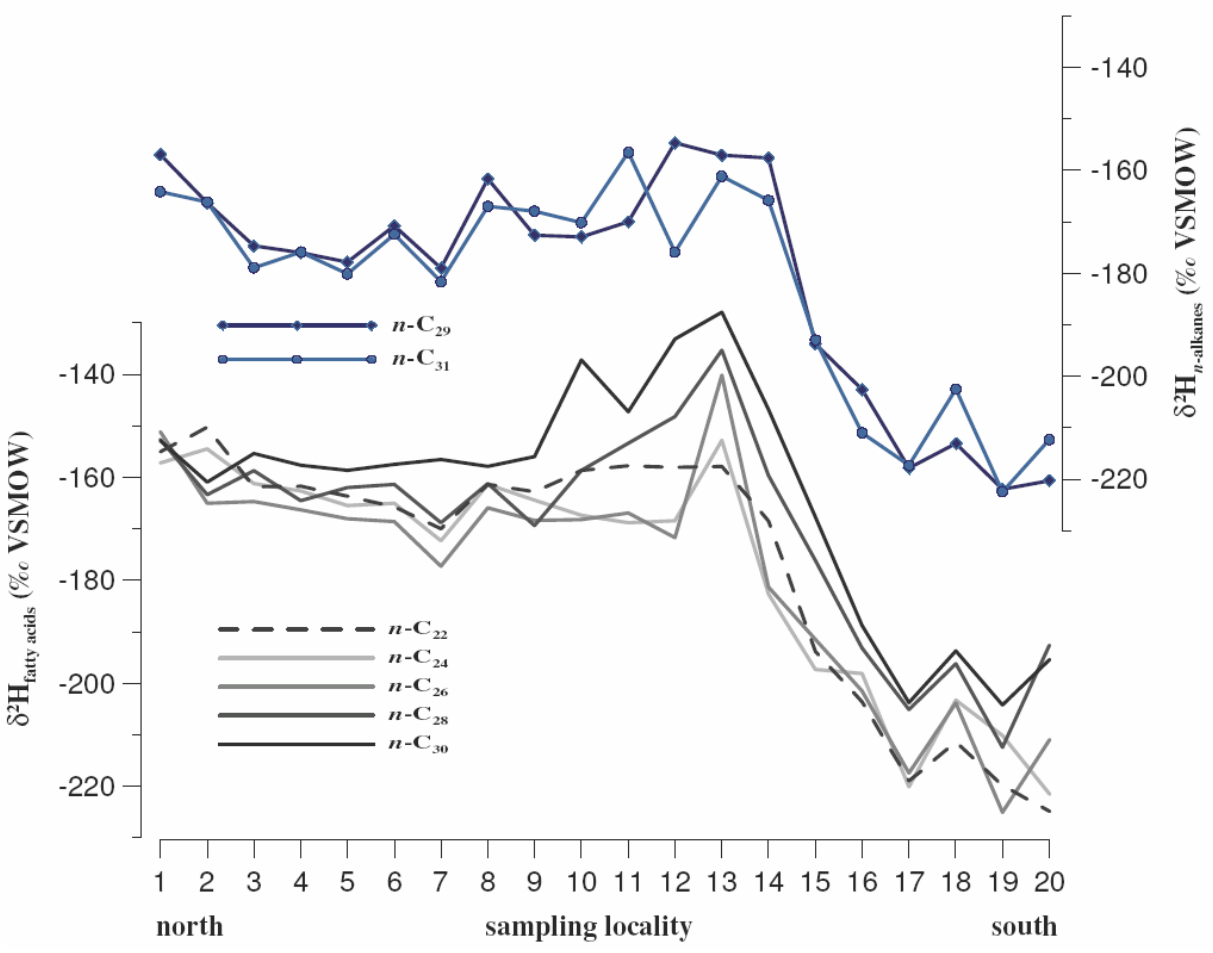

693

694 **Fig. 2:** Comparison of δ^2H results of individual leaf wax *n*-alkanes and *n*-alkanoic (fatty)

695 acids along the investigated transect.

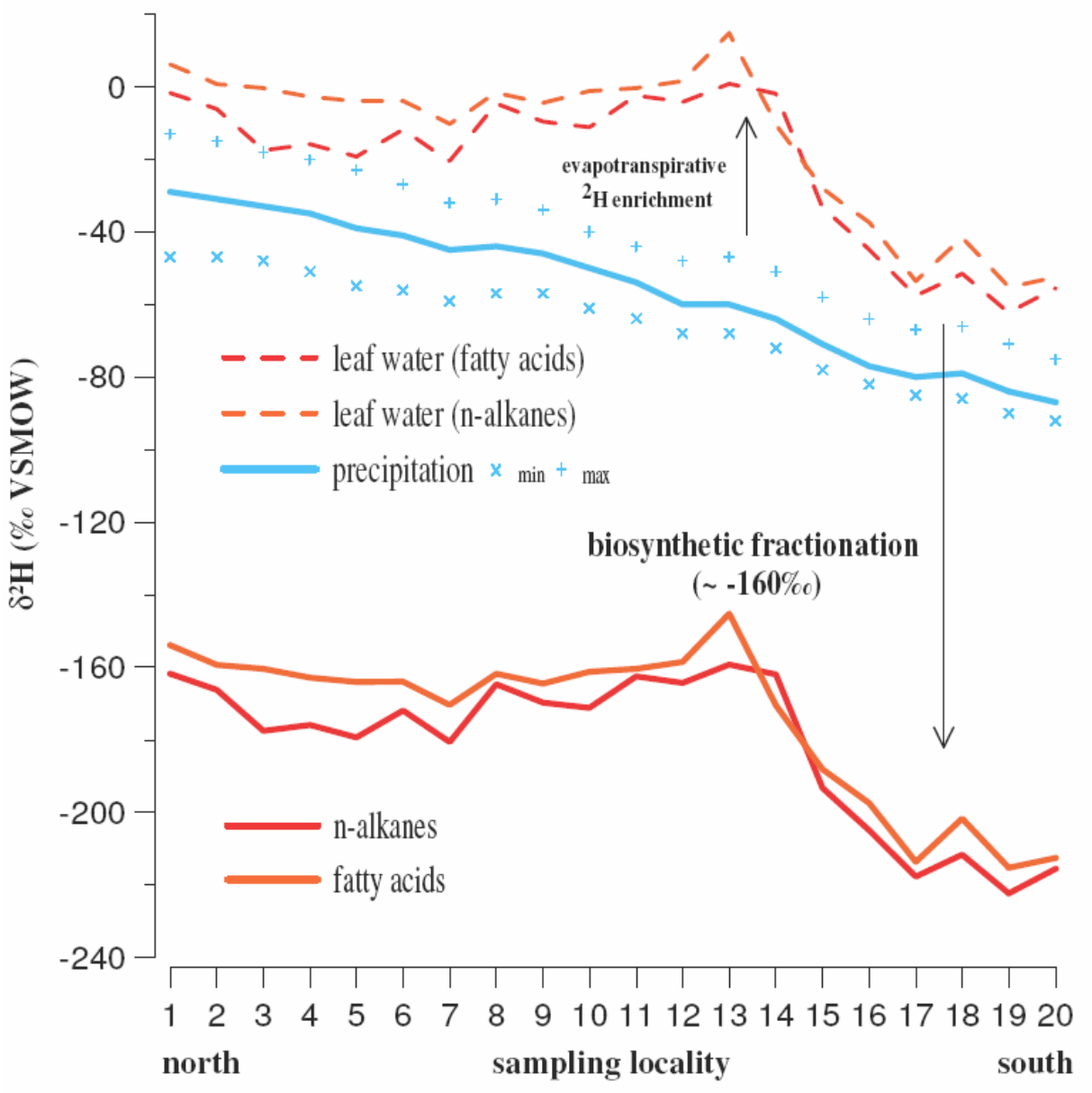

Fig. 3: Comparison of measured $\delta^2H_{n\text{-alkanes}}$ (weighted mean of n-C_{29} and n-C_{31}) and $\delta^2H_{fatty\ acids}$ (weighted mean of n-C_{22}, n-C_{24}, n-C_{26}, n-C_{28} and n-C_{30}) pattern with δ^2H_{prec} (Bowen, 2012) along the north-south climate transect (^{x}min and $^{+}$max representing annual minimum and maximum value at the sampling site). Additionally, assuming a biosynthetic fractionation of -160 ‰ for the n-alkane and fatty acid biosynthesis in plants the biomarker-based 'reconstructed' isotopic composition of leaf water is shown.

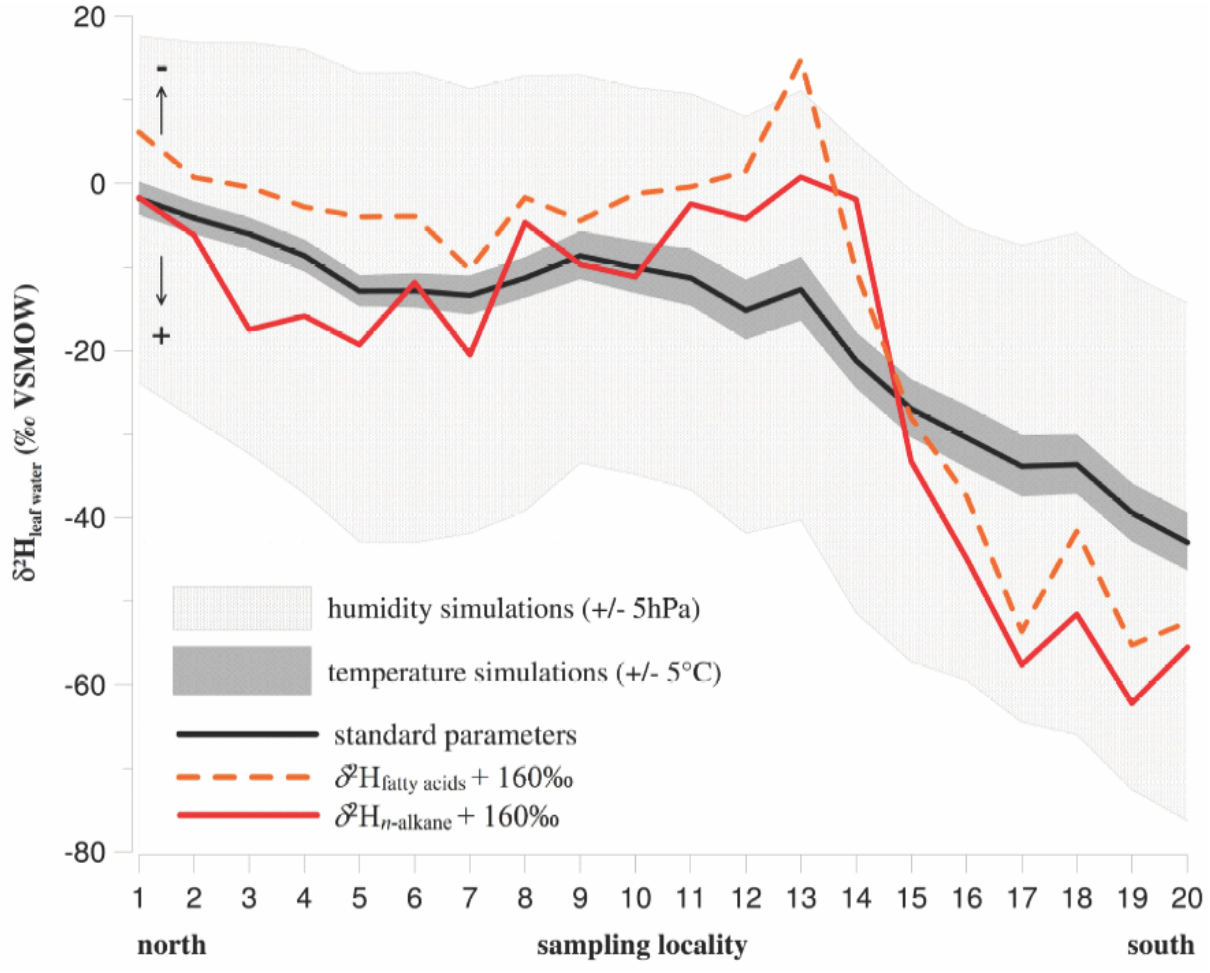

Fig. 4: Results of $\delta^2H_{leaf\ water}$ model simulations and comparison with biomarker-based 'reconstructed' (assuming a biosynthetic fractionation factor of -160 ‰) isotopic composition of leaf water based on *n*-alkanes and fatty acids, respectively. Sensitivity tests for $\delta^2H_{leaf\ water}$ are shown for changes in RH and air temperature for all 20 sites along the transect.

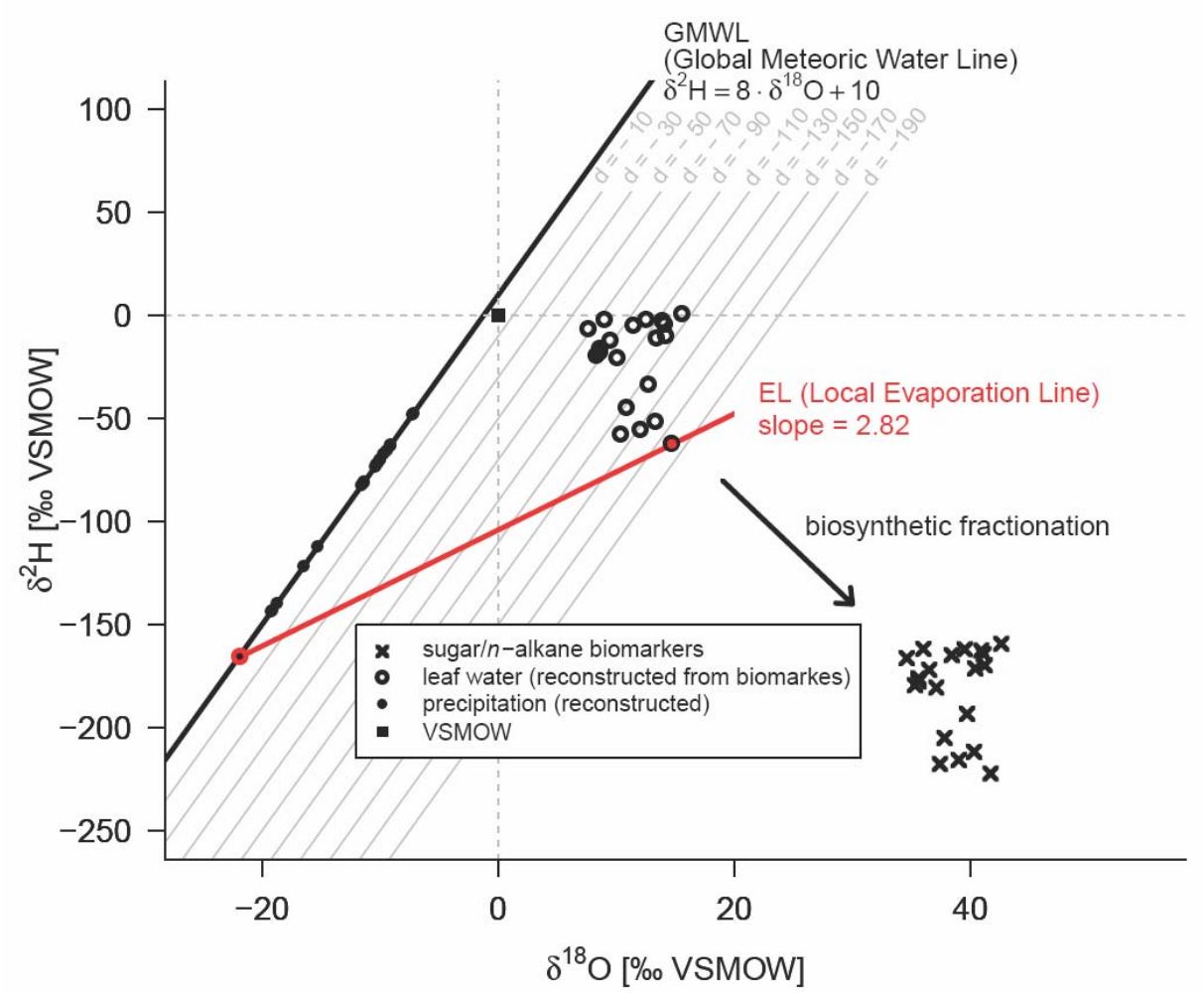

710

711 **Fig. 5:** $\delta^{18}O$-$\delta^{2}H$ diagram illustrating the conceptual model of the coupled $\delta^{2}H_{n\text{-alkane}}$-$\delta^{18}O_{sugar}$

712 approach (modified after Zech M. et al., 2013a). $\delta^{2}H_{n\text{-alkane}}$ (mean of n-C_{29} and n-C_{31})

713 and $\delta^{18}O_{sugar}$ (mean of arabinose, fucose and xylose) results are used to reconstruct

714 $\delta^{2}H/\delta^{18}O_{leaf\ water}$ by subtracting the biosynthetic fractionation factors. The deuterium

715 excess ($d = \delta^{2}H - 8 \cdot \delta^{18}O$) of leaf water serves as proxy for RH and $\delta^{2}H/\delta^{18}O_{prec}$ is

716 calculated as intersection of the individual evaporation lines (ELs, slope 2.82) with the

717 global meteoric water line (GMWL).

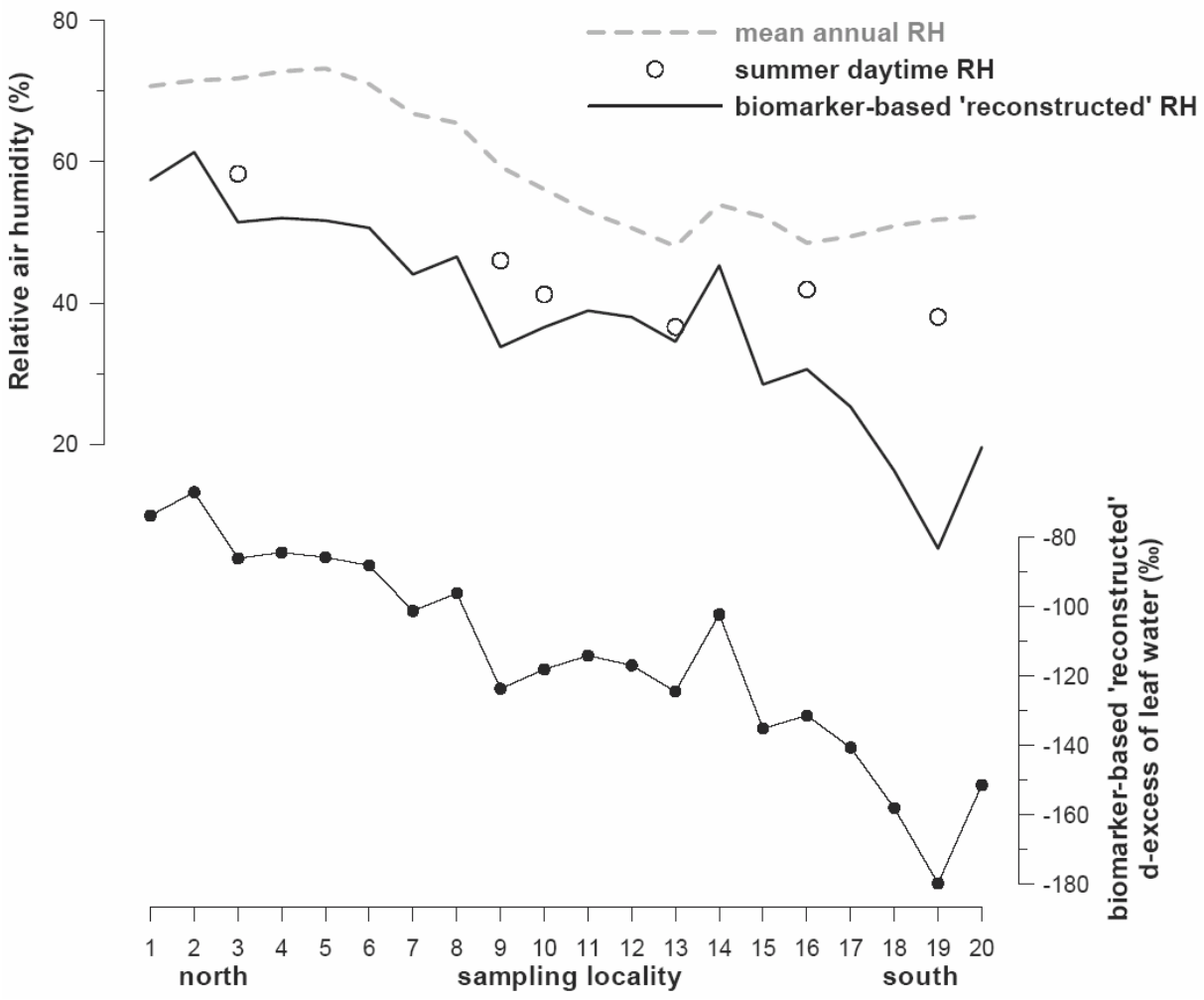

718

719 **Fig. 6:** Comparison of biomarker-based 'reconstructed' relative humidity (RH) values with
720 actual RH values (mean annual RH retrieved for all investigated sites from GeoINTA,
721 2012; summer daytime RH for six stations retrieved from www.ncds.noaa.gov).
722 Deuterium excess values were calculated using $\delta^{18}O_{leaf\ water}$ reconstructed from
723 terrestrial sugars (Tuthorn et al., 2014) and $\delta^{2}H_{leaf\ water}$ reconstructed from *n*-alkanes.

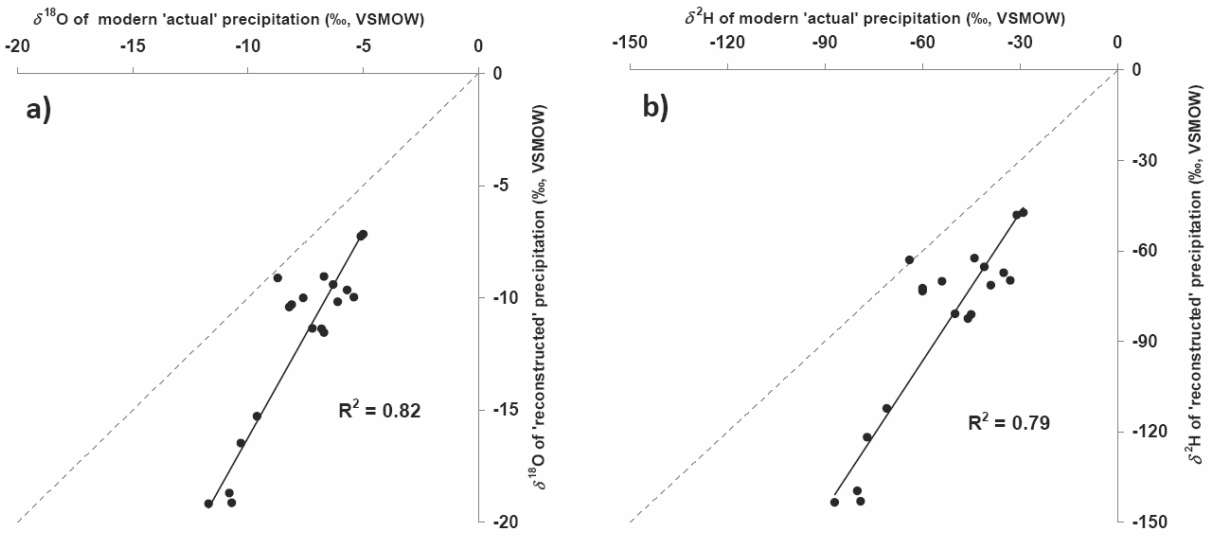

724

725 **Fig. 7:** Correlation of biomarker-based 'reconstructed' $\delta^{18}O_{prec}$ and $\delta^{2}H_{prec}$ values with

726 modern 'actual' $\delta^{18}O_{prec}$ and $\delta^{2}H_{prec}$ values (from Bowen, 2012).